# Seismic response analysis of nuclear power plant founded on sliding elastomer bearing pads

K.Uchida, K.Emori, K.Mizukoshi & Y.Takenaka
*Kajima Corporation, Tokyo, Japan*
J.Betbeder-Matibet
*Electricité de France, Paris*
J.-P.Noël-Leroux & P.Uhrich
*Spie Batignolles, Vélizy-Villacoublay, France*



## 1 INTRODUCTION

Introduction of base isolation concept to the seismic design of nuclear power plant (NPP) has recently been expected in Japan as an effective measure to reduce drastically the seismic force for both buildings and equipement and piping. An analytical study on earthquake response of a French type base isolation system for NPP is carried out as a joint study between Kajima Corporation of Japan and Électricité de France (EDF) and Spie Batignolles (SB) of France. The purpose of this study is to grasp the seismic behavior of a base-isolated NPP using the sliding elastomer bearing pads (hereafter referred to as "aseismic bearings") which were developed and actually applied to Koeberg NPP in South Africa by EDF and SB (Jolivet & Richli 1977, et al.), and to evaluate the feasibility of application of the base isloation system in Japan.

In this base isolation system, a pair of friction plates of each aseismic bearing can slip relative to each other when the horizontal shear force reaches a level of friction force. And it is anticipated that, during earthquake, the friction force level may fluctuate every moment and every location with the fluctuation of contact force applied to the friction plates. In this study, the base-isolated structure is modeled as a two dimensional multi-stick lumped-mass model in which the flexibility of the upper and lower rafts is taken into account and the aseismic bearings are modeled as fourteen nonlinear elements being capable of expressing above-mentioned complex sliding phenomenon of friction plates caused by fluctuating contact force. Using this model, a series of nonlinear earthquake response analyses are perfomed by applying horizontal and vertical earthquake ground motions simultaneously. And then, the dynamic behavior of the base-isolated reactor buildings and aseismic bearings are clarified , and the effectiveness of the system is discussed in comparison with the response of a non-isolated buildings.

## 2 OUTLINE OF BASE ISOLATION SYSTEM

The base-isolated NPP treated in this paper is a standard twin units French PWR 900MW, CP1 type, which consists of two reactor buildings, two fuel storage buildings, two connecting buildings, one electrical building, and one nuclear auxiliary building which are constructed on

a common upper raft (149 m x 86 m) to form a "nuclear island" weighing about 390,000 tons. The nuclear island is supported by a lower raft founded on the bedrock through about 2000 aseismic bearings.

The basic concept of the base isolation system is shown in Fig.1. Low intensity earthquakes only cause linear distortion of the laminated elastomer pads, and high intensity earthquakes cause both distortion of the laminated elastomer pad and slippage between the friction plates. The system thus works as a filter which transmits no shear force larger than the friction force to the upper buildings. The detail of the laminated elastomer is shown in Fig.2.

## 3 ANALYTICAL MODEL

The NPP is assumed in this study to be built on a hard rock site (shear velocity Vs = 1,500 m/s) without embedment.

As shown in Fig.3, the buildings and upper and lower rafts are modeled as a two dimensional multi-stick lumped-mass model representing the nuclear island in the longitudinal direction in which each mass point has three degrees of freedom, namely vertical, horizontal and rotational directions. For the building structures, the Rayleigh type damping with 5% of critical damping at both 0.9Hz and 10Hz is assumed.

The upper and lower rafts are connected with each other using fourteen non-linear elements (refer to Fig.4) representing in the plane a half of the aseismic bearing rows. Assumed for these non-linear elements is the internal viscous type damping with 5% at 0.9Hz for the horizontal deformation and 7% at 12Hz for the vertical deformation. As for the Coulomb friction elements representing the friction plates, the two states depending on the occurrence of the slippage are considered as follows;

$$\text{Non-slip state:}\quad Fs = Ks\,(\Delta s - \Delta r) + Cs\,\dot{\Delta}s$$
$$Fv = Kv\,\Delta v + Cv\,\dot{\Delta}v$$
$$\text{Slipping state:}\quad Fs = \mu Fv\,\mathrm{sgn}(\dot{\Delta}s)$$
$$Fv = Kv\,\Delta v + Cv\,\dot{\Delta}v$$

where
- Fs, Fv; Shear (friction) force, contact force
- Ks, Kv; Horizontal and vertical stiffnesses
- Cs, Cv; Horizontal and vertical damping coefficients
- $\Delta s$, $\Delta v$; Horizontal and vertical deformations
- $\Delta r$; Accumulated slip amount
- $\mu$; Coulomb friction coefficient ( = 0.2)

The condition for the change from non-slip state to slipping state is expressed as "$|Fs| \geq \mu Fv$"

Each mass point of the lower raft is supported by vertical and horizontal Winkler-type soil springs representing elastic deformation of the ground. The soil spring is estimated from static stiffness of semi-infinite elastic soil medium assuming that the vertical or horizontal reaction force to the soil surface is uniform. The internal viscous type damping is assumed for the soil springs considering radiation effect, where the damping factors of 2.3% and 26% are given at the horizontal and vertical fundamental frequencies (0.9Hz and 8.7Hz), respectively.

## 4 EIGENVALUE ANALYSIS

The natural frequencies and participation factors of the linear model for the isolated building, where the slippage of friction plates is restricted, are shown in Table 1, and Fig. 5 shows its typical mode shapes. For comparison, the natural frequencies of the non-isolated building are shown in Table 2.

As to horizontal input, only the mode at 0.89Hz in which the overall nuclear island moves horizontally as a rigid body predominates for the isolated building, in contrast with the non-isolated building having the higher modes with relatively large participation factors. As to vertical input, several predominant modes accompanying with local deformations of the upper and lower rafts appear in the range of 8 to 10Hz.

## 5 EARTHQUAKE RESPONSE ANALYSIS

### 5.1 Input Earthquake Ground Motions

As shown in Table 3, the El Centro 1940 NS and UD waves and the synthesized waves for the far field S2 earthquake are used as the input ground motions for the response analysis. The response spectra of these ground motions are shown in Fig.6. The S2 earthquake is the wave proposed by the "Seismic Design Sub-committee of MITI on Improvement and Standardization of Light Water Reactor" of Japan.

The analytical cases presented herein are shown in Table 4.

### 5.2 Response of Buildings

The horizontal response acceleration time histories obtained from the analysis show that the response of the isolated building has a smaller quantity of high frequency component than that of the non-isolated building. The isolated buildings oscillate mainly at the fundamental frequency of 0.89Hz, and the acceleration amplification in the direction of height is small.

The maximum responses of the reactor building (R/B) are shown in Fig.7. As was expected, the isolated buildings have much smaller horizontal acceleration and shear force, but conversely larger horizontal displacement, than the non-isolated buildings. The responses in the vertical direction against the same wave are almost the same for isolated and non-isolated buildings (Cases 1 and 3).

Fig.9 shows the horizontal acceleration floor response spectra for the damping factor of 1% at the points A and B shown in Fig.8. The spectral values are markedly reduced by introducing the base isolation in the frequency range higher than 2Hz, which may result in a great advantage for the aseismic design of equipment and piping.

### 5.3 Response Behavior of Aseismic Bearings

The horizontal shear force vs. displacement hysteresis loops of the aseismic bearings at the typical locations are shown in Fig.10. It is found that the hysteresis loop pattern differs depending on its location, which results in making the maximum and residual slippage of friction plates as well as residual shear deformation of elastomer after earthquake be uneven depending on its location.

Fig.11 shows the distribution of the maximum response values of the

fourteen aseismic bearing elements in the model. The variation of contact force which is shown as shaded region in Fig.11(a) is not uniform but not large enough to cause uplift. Fig.11(b) indicates that the horizontal relative displacement between the upper and lower rafts is a litte less than 10 cm and is uniformly distributed due to the large in-plane stiffness of the upper raft, but, the maximum and residual slippage between friction plates is not uniform because of the uneven variation in contact force as shown above. Fig.11(c) shows the residual horizontal deformation of elastomers after earthquake which variate within 2cm depending on the location.

## 6 CONCLUDING REMARKS

As the results of the analyses, the dynamic response behavior of the base isolated buildings and aseismic bearings during earthquakes are clarified. Especially, it is suggested that all aseismic bearings throughout the foundation do not necessarily behave uniformly because of the uneven fluctuation of the contact force applied to the friction plates during earthquakes.

In spite of such local complex behavior of each aseismic bearing, it is also shown from analytical results that the response acceleration, shear forces and floor response spectra of the reactor building are markedly reduced in comparison with a non-isolated building. Furthermore, it is confirmed that no uplift nor excessive slippage between friction plates are caused even under S2 earthquake specified in Japan.

## REFERENCES

Jolivet, F. and Richli, M. 1977. Aseismic foundation system for nuclear power stations. Proc. 4th SMiRT. K9/2

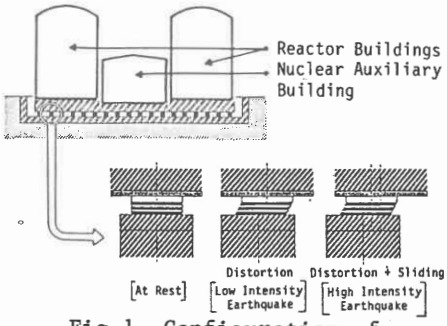


Fig.1 Configuration of Base-isolated N.P.P.

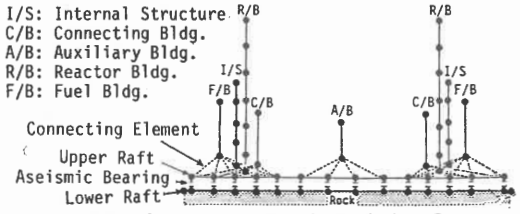


Fig.3 Analytical Model of Isolated Building

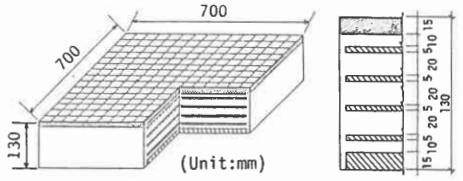


Fig.2 Detail of Aseismic Bearing

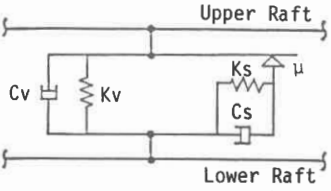


Cv: Vertical Damping Coef.
Kv: Vertical Stiffness
Cs: Horizontal Damping Coef.
Ks: Horizontal Stiffness
μ: Coef. of Friction

Fig.4 Non-linear Element for Aseismic Bearing

Table 1 Eigenvalues of Isolated Building

| Mode | Freq. (Hz) | Participation Factor Horiz. $\beta_x$ | Vert. $\beta_y$ | Note |
|---|---|---|---|---|
| 1 | 0.891 | 1.0746 | 0.0003 | Overall Horiz. Motion |
| 2 | 3.65 | 0.0141 | 0.0348 | R/B Horizontal 1st |
| 3 | 4.10 | 0.0863 | 0.0365 | R/B Horizontal 2nd |
| 4 | 5.02 | 0.0025 | 0.0303 | |
| 5 | 5.41 | 0.0189 | 0.0342 | |
| 6 | 6.36 | 0.0008 | 0.0131 | |
| 7 | 6.51 | 0.0005 | 0.0382 | |
| 8 | 7.26 | 0.0021 | 0.0050 | |
| 9 | 7.32 | 0.0012 | 0.0928 | |
| 10 | 8.03 | 0.0202 | 0.2467 | |
| 11 | 8.70 | 0.0026 | 1.7591 | Overall Vert. Motion |
| 12 | 9.06 | 0.0064 | 0.2660 | |
| 13 | 10.0 | 0.0001 | 0.2539 | |
| 14 | 10.1 | 0.0001 | 0.3712 | |

Table 2 Eigenvalues of Non-isolated Building

| Mode | Freq. (Hz) | Participation Factor Horiz. $\beta_x$ | Vert. $\beta_y$ | Note |
|---|---|---|---|---|
| 1 | 3.74 | 2.1331 | 0.0117 | R/B Horizontal 1st |
| 2 | 3.86 | 1.7727 | 0.0441 | R/B Horizontal 2nd |
| 3 | 5.13 | 0.8053 | 0.0108 | |
| 10 | 9.33 | 0.2124 | 1.9115 | Overall Vertical Motion |

Table 3 Input Ground Motions

| Name | Horizontal Max. Acc. | Vertical Max. Acc. | Duration |
|---|---|---|---|
| El Centro 1940 | 341.70Gal | 206.30Gal | 16.0sec |
| $S_2$ (M=8.5, Δ =68km) | 407.10Gal | 217.15Gal | 40.0sec |

Table 4 Analysis Cases

| Case | Foundation | Input Ground Motion | Analysis |
|---|---|---|---|
| Case 1 | Isolated | El Centro 1940 | non-linear |
| Case 2 | Isolated | $S_2$ (M=8.5, Δ =68km) | non-linear |
| Case 3 | Non-isolated | El Centro 1940 | linear |

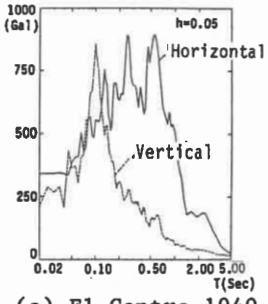


(a) El Centro 1940

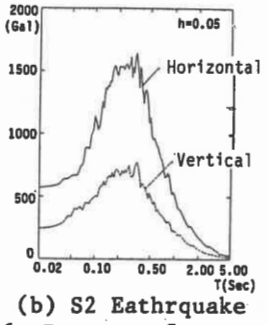


(b) S2 Eathrquake

Fig.6 Response Spectra of Input Ground Motion

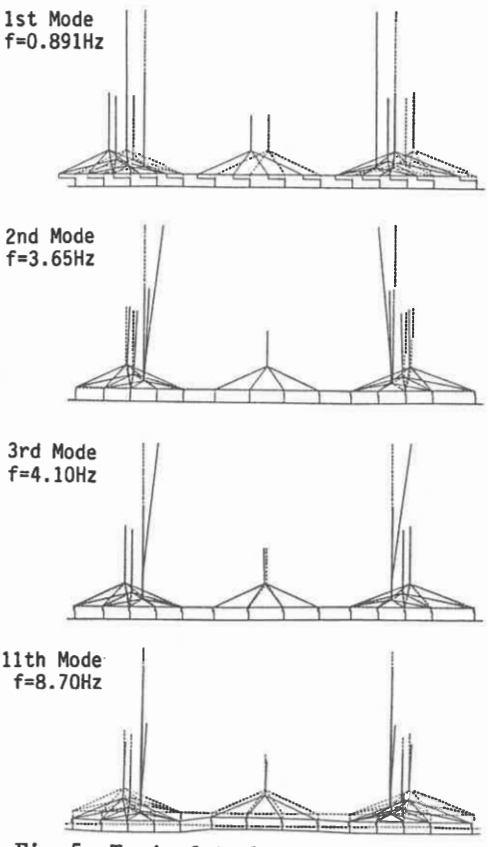


Fig.5 Typical Mode shapes of Isolated Building

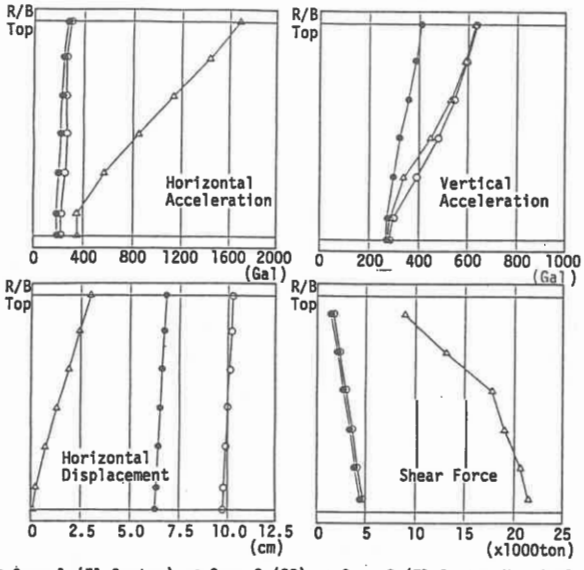


○ Case 1 (El Centro) ● Case 2 (S2) △ Case 3 (El Centro Non-isolated)

Fig.7 Maximum Response of Unit 1 R/B

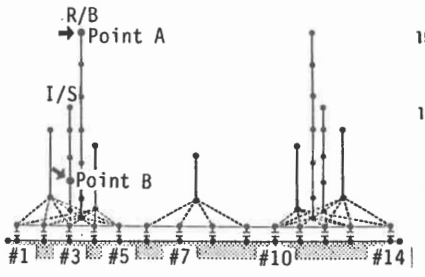


Fig.8 Location of Output

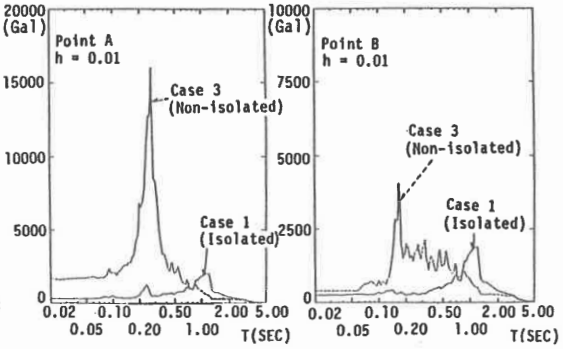


Fig.9 Horizontal Floor Response Spectra (Case 1, Case 3, El Centro)

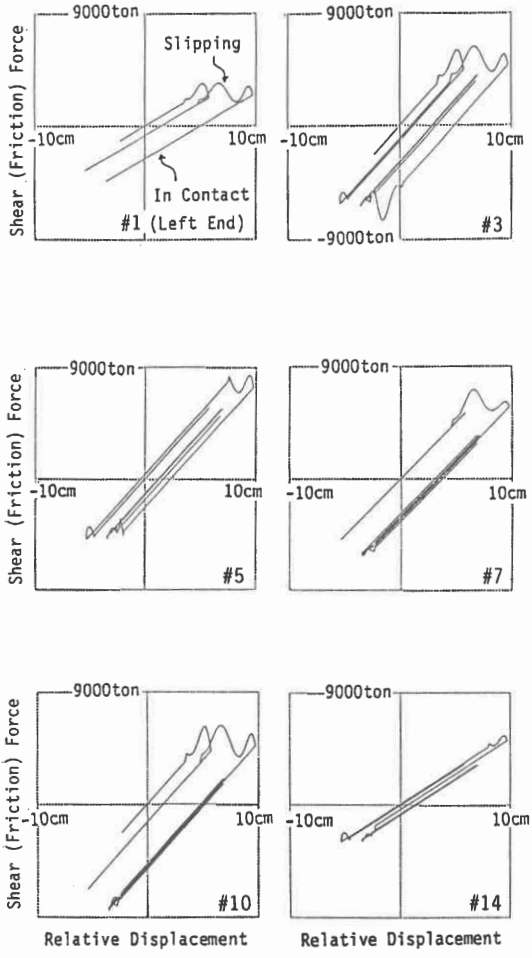


Fig.10 Histeresis Loop of Aseismic Bearings (Case 1, El Centro)

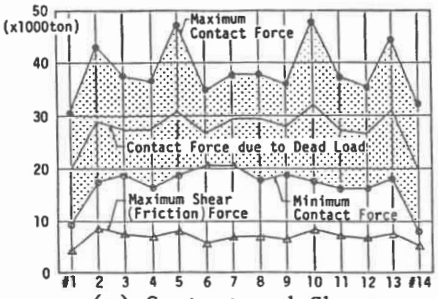


(a) Contact and Shear (Friction) Force

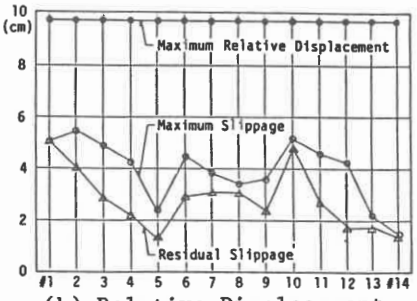


(b) Relative Displacement and Slippage

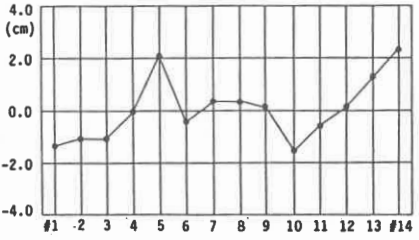


(c) Residual Deformation of Elastomer

Fig.11 Response of Aseismic Bearings (Case 1, El Centro)